LA-UR- 96-1945

CONF-9606233--1

Title: The Application of a Microstrip Gas Counter to Energy-Dispersive X-Ray Fluorescence Analysis

Author(s): R. E. Morgado
J. F. C. A. Veloso
J. M. F. dos Santos
C. A. N. Conde

Submitted to: EDXRS-96 Conference
Lisbon, Portugal
June 23-28, 1996

DISCLAIMER

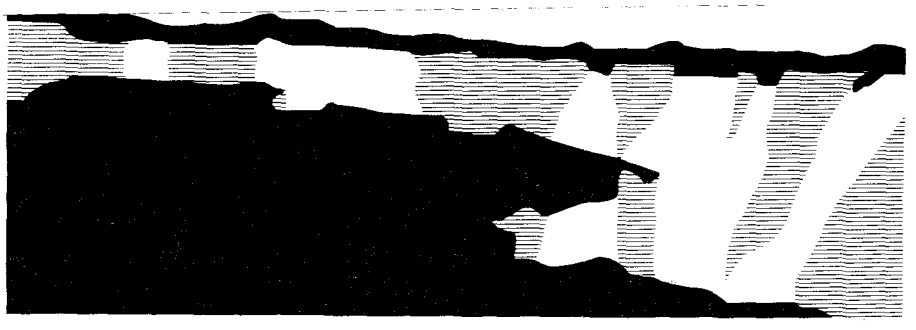

Los Alamos
NATIONAL LABORATORY

Form No. 836 R5
ST 2629 10/91

The Application of a Microstrip Gas Counter to Energy-Dispersive X-ray Fluorescence Analysis

J. F. C. A. Veloso, J. M. F. dos Santos, and C. A. N. Conde
Departamento de Física da Universidade de Coimbra
Combra P3000 Portugal
and
R. E. Morgado
Los Alamos National Laboratory
Los Alamos, New Mexico 87545
USA

ABSTRACT

Performance characteristics of a microstrip gas counter operated as a x-ray flourescence spectrometer are reported. Gas amplification as a function of microstrip anode-cathode voltage was measured, and the breakdown threshold voltage was determined in pure xenon. The detector temporal stability and the effect of gas purity were assessed. Energy resolution and linearity, detection efficiency, and uniformity of spatial response in the 2- to 60-keV x-ray energy range were determined from the pulse-height distributions of the fluorescence x-ray spectra induced in a variety of single- and multi-element sample materials. Energy resolution similar to conventional proportional counters was achieved at 6 keV.

I. INTRODUCTION

Since its introduction by Oed in[1] 1988, the microstrip gas counter (MSGC) has developed rapidly with applications in diverse fields, such as medicine[2,3], high energy physics[4,5] and x-ray astronomy[6,7]. The MSGC is a miniaturized, planar variant of the multiwire proportional chamber in which wires have been replaced by closely-spaced metal electrode strips deposited on an insulating substrate. It is a high-resolution, compact detector with high-rate capability, stable gain, inherent spatial sensitivity, and reduced space-charge effects. In principle, it can be fabricated into any desired geometric configuration and size.

MSGCs have been operated in a variety of filling gases. Our interest in pure xenon stems from an earlier work [8] in which we reported our experiences with a MSGC that was vacuum-coated with a thin layer of photocathode material (CsI) and used as the vacuum ultraviolet (VUV) photosensor in a xenon gas proportional scintillator counter (GPSC). In this earlier application, the MSGC was co-located within the xenon gas envelope of the GPSC to detect photoelectrons

ejected from the CsI photocathode by the VUV photons from xenon scintillation. The results, although encouraging for a first attempt, were less than optimum. Since we intend to continue developing the MSGC as a photosensor for a GPSC, we now seek a better understanding of the basic performance characteristics of a MSGC operated in pure xenon without the additional complication of photoelectron production.

To more fully appreciate the results of our earlier experiences, we have determined the characteristics of a MSGC when it is used to detect the primary electrons from the absorption of x-rays in pure xenon. These include the gas multiplication as a function of the MSGC voltages up to the discharge threshold and the variation in gas gain with time and gas purity.

We also report the performance of a MSGC operated in pure xenon as an energy dispersive x-ray flourescence spectrometer. The energy linearity and resolution in the x-ray energy range between 2 and 60 keV were determined from the measured x-ray fluorescence pulse-height spectra induced in a variety of single- and multi-element target samples.

II. DESCRIPTION

A. Experimental apparatus

A cross section of the detector design developed for this study is depicted schematically in Figure 1. Incident x-rays are absorbed in the 3-mm absorption/drift region located between the entrance window and the microstrip detector plate. The primary ionization forms an electron cloud which drifts into the sensitive volume of the microstrip detector under the influence of the uniform field between the window and the microstrip detector. Amplification of the signal results from the electron avalanche in the high field in the immediate region of the microstrip anodes.

Particular attention was directed to the selection of component materials and in the maintenance of cleanliness during the fabrication and assembly processes. Indium gaskets are used throughout to form vacuum seals and the microstrip detector plate is located by four standoffs fabricated from Macor (Corning Glass Works), a machinable glass ceramic. Stainless-steel contacts make up the internal electrical connections while external connections are routed through a welded glass-metal multi-pin feedthrough connector. The 125-μm aluminized Kapton (a DuPont polyimide film) entrance window and the detector envelope are maintained at ground potential .

The microstrip plate (MSP) is a 30x30 mm^2 CERN model MS-4 produced by Baumer Industries of Switzerland. The MSP consists of 10-μm anodes and 80-μm cathodes at a 200-μm pitch, composed of 0.2-μm of chromium deposited on a 500-μm Desag D263 glass substrate.

The backplane is a flat, unstructured layer of 0.1-μm chromium. For all the results reported here, the backplane and cathodes were maintained at ground potential while a positive voltage, V_{ac}, was applied to the anodes.

The detector was operated at one atmosphere of pure xenon, purifed continuously in normal operation by convection through SAES ST707(150°) getters. For the gas ageing tests, the plumbing of the gas system was routed to either include or exclude the purfication branch.

B. Data Acquisition and Analysis Systems

Anode pulses were preamplified by a HP5554 (1000 mV/pC sensitivity), linearly amplified by a HP5582A operated with 5-μs first differentiation, no second differentiation, and a 5-μs integration time, and analyzed according to pulse height by a Nucleus PCAII whose ADC was operated with a 1024-channel gain. The peak amplitudes and energy resolution of the measured pulse-height distributions were obtained by fitting the measured distributions with a gaussian function superimposed on a linear background[10].

III. OPERATIONAL CHARACTERISTICS

All of the characteristics evaluated in this section were measured with the 5.9-keV x-ray from a ^{55}Fe source equipped with a 1-mm diameter collimator which limited the incident flux to 10^2 $s^{-1}mm^{-2}$. These included the gas gain and stability as functions of time, voltage, and gas purity, and the electrical breakdown threshold, energy resolution, spatial uniformity, and detection efficiency.

A. Gas gain

The variation of the absolute gas gain as a function of anode-cathode voltage, V_{ac}, is depicted in Figure 2. The variation is exponential as might be expected and electrical breakdown was observed at V_{ac} ~520 V, corresponding to a maximum gas gain of approximately 10^4.

The MSGC absolute gain was obtained by determining the absolute gain of a standard proportional counter operated under the same conditions, according to the procedure described in Ref.11. To monitor the proportional counter absolute charge gain during anode signal data acquisition, a signal of known amplitude from a pulse generator (BNC PB-3) was fed into the test imput of a HP 5554A charge sensitive preamplifier through a 1.0 pF capacitor.

B. Anode Voltage Plateau

The counting rate as a function of anode voltage is depicted in Figure 3. A plateau is reached at an applied voltage of ~420 V, with $V_b=V_c=V_d=0$, where b, c, d, represent the backplane,

cathode, and, respectively. Thus, the V_{ac} region for the best MSGC energy resolution is already on the plateau.

C. Energy resolution

Energy resolution (also depicted in Figure 2) continues to improve with increasing anode-to-cathode voltage until V_{ac} is approximately equal to 440V, above which a degradation in the energy resolution is visible. The best energy resolution, according to Figure 2, was achieved with V_{ac} between 430 and 450 V, corresponding to a more modest gain of $2\text{-}3x10^3$.

The observed rapid degradation of the energy resolution at higher anode-cathode voltages is most likely attributable to two mechanisms which result in additional spurious electrons. Electrons may be produced in the high-field regions near the cathode strips which can be intense enough to extract electrons from the cathode surface by field emission. In addition, the absence of any ultraviolet quenching agents in the sensitive gas volume will permit the production of VUV scintillation photons from xenon, leading to a positive-feedback situation. The scintillation photons may strike the microstrip electrodes and detector walls and eject photoelectrons into the gas volume.

D. Gas gain stability over time

The centroid positions were determined for the 5.9-keV x-ray pulse-height distributions measured by the multichannel analyzer and plotted in Figure 4 as a function of time for two-minute acquisition periods for each data point. Following an intial rapid decrease, detector gain stabilizes after 4 to 6 hours. This behavior can be attributed to positive ion buildup on the surface of the insulating microstrip plate substrate (Desag D263 glass), which leads to a continuous reduction in the intensity of the electric field near the anode until equilibrium is achieved. Detector gain stability was achieved after a time that depended on the incident flux, as illustrated in Figure 4, while energy resolution was not observed to change with time under similar conditions .

E. Gas purity

In order to evaluate the effects of gas purity on detector gain and energy resolution, both parameters were monitored as functions of time with the gas purification branch either included in or excluded from the gas circulating system. Again, the centroid positions were determined for the 5.9-keV x-ray pulse-height distributions measured by the multichannel analyzer and plotted in Figure 5 as a function of time for two-minute acquisition periods for each data point..

The detector output signal was monitored for two days after gas circulation through the purifying getters was interrupted. With the gas purification branch closed, the detector was turned off for five more days before being switched on again. After several minutes, the gas purification branch was reopened.

According to Figure 5, continuous gas purity is important to the stability of the detector gain over time. After discontinuing purification (Figure 5a), detector gain decreases steadily with time and does not stabilize, as it would under normal operating conditions with gas purification (see Figures 4 and 5b).

The effect of gas purity on detector energy resolution is much less than the effect on detector gain. The detector energy resolution degrades slowly with time, increasing from about 16% to about 20% over a period of approximately 7 days.

Once gas purification was resumed, detector gain and energy resolution resumed their initial values and stabilized within a few hours, as illustrated in Figure 5b. The newer stabilized values are slightly different from the initial values because a different area of the detector was exposed. As explained in the next section, the measured variations in detector spatial uniformity is larger than the variations due to gas purity.

F. Spatial uniformity

The variation in microstrip plate gain along two orthogonal directions, normal and parallel to the electrode strips, was studied to determine the spatial uniformity. In Figure 6 the centroid of the 5.9-keV x-ray pulse-height distribution, measured along both directions with a 1-mm collimated beam, are presented. Pulse-height-amplitude variations as large as 10% can occur, leading to an overall degradation of the energy resolution as a function of detector window size. However, the energy resolution for the 5.9-keV K_α fluorescence line from a Mn target was not significanlty degraded in the more uniform central region of the microstrip plate when a 10-mm diameter entrance window was used.

G. Detection Efficiency

The operational characteristics of a MSGC are unaffected, to first order, by the depth of the absorption/drift region. Consequently, detection efficiency can be improved by increasing the depth of this region. To test this hypothesis, a MSGC with a 5-cm deep absorption/drift region was fabricated and, in initial testing, the same MSGC operational characteristics were obtained.

The choice of a 3-mm absorption/drift region at one atmosphere of pure xenon limits the detection efficiency in the present design. The detection efficiency for x-ray energies up to 2.4

keV is greater than 90%, for energies up to 8 keV it is greater than 40%, and for 25 keV it is 2%. However, in the soft x-ray region, detection efficiency is determined by the transparency of the radiation window. In the present case, the 125-μm Kapton window transmits 10% of the x-rays with energies of at least 3 keV, 50% at 5 keV, and 90% at 10 keV.

IV. X-RAY FLUORESCENCE SPECTROMETRY

The energy linearity of the MSGC detector was determined in the 2- to 60-keV x-ray energy range using the fluorescence radiation induced in both single-element and multi-element target samples. Samples were positioned 10 mm from the detector window and flourescence was induced by ^{241}Am, ^{244}Cm, or ^{55}Fe x-ray sources equipped with 10-mm diameter collimators.

A. Single-element Target Samples

Single-element targets included pure samples of Cl, Ca, Cr, Mn, Fe, Ni, Cu, Zn, Nb, Cd, Sn, Ba, Dy. The centroids and full-width-half-maxima (FWHM) of the measured pulse-height distributions are plotted in Figure 7a as a function of x-ray energy. As expected, good energy linearity is maintained throughout the energy range. Energy resolution is also approximatly linear with $E^{-1/2}$, as illustrated in Figure 7b.

The pulse-height distributions of ^{241}Am, ^{244}Cm and ^{55}Fe sources, measured directly in the detector, are shown in Figures 8a, b, and c, respectively.

B. Multi-element Target Samples

X-ray flourescence spectra were measured for muscovite ($KAl_2(AlSi_3)O_{10}(OH)_2$), portland cement, non-homogeneous pyrite/chalcopyrite, lead, and SAES ST707 getters (70% Zr, 5.4% Fe, and 24.6% V). The resulting pulse-height distributions are depicted in Figures 9a, b, c, d and e, respectively. The results are similar to what would be obtained with a pure xenon proportional counter.

VI. CONCLUSIONS

The performance characteristics of a microstrip gas counter operated as a x-ray flourescence spectrometer have been determined in pure xenon. Gas amplification as a function of the anode-cathode voltage, detector ageing, and gas purity have been measured, and the breakdown threshold voltage determined. Energy resolution and linearity, detection efficiency, and uniformity of spatial response in the 2- to 60-keV x-ray energy range were determined from the pulse-height distributions of the fluorescence x-ray spectra induced in a variety of single- and

multi-element sample materials. Energy resolution similar to conventional proportional counters was achieved in the specified energy range.

Compared to conventional proportional counters, the MSGC is more compact, can be produced with large sensitive areas, and achieves comparable energy resolution. In applications to energy-dispersive x-ray fluorescence (EDXRF) analysis, the MSGC is a viable candidate for replacing the conventional proportional counter.

Development will continue to focus on improving the overall performance characteristics of a MSGC both as the signal amplification device in a xenon proportional counter and as the photosensor for a gas proportional scintillator counter.

REFERENCES

1 A. Oed, "Position-sensitive Detector with Microstrip Anode for Electron Multiplication with Gases," Nucl. Instrum and Meth., A263 (1988) 351-359.

2 F. Sauli, "Applications of gaseous detectors in astrophysics, medicine and biology," Nucl. Instrum. and Meth., A323 (1992)1-11.

3 E. A. Babichev et al. (12 authors), " High pressure multiwire proportional and gas microstrip chambers for medical radiology," Nucl. Instrum. Meth., A360 (1995) 271-276.

4 F. Angelini, R. Bellazzini, A. Brez, G. Decarolis, C. Magazzù, M. M. Massai, G. Spandre and M. R.Torquati, "Results of the First use of Microstrip Gas Chambers in High-energy Physics Experiments" Nucl. Instrum. Meth. A315(1992)21-32.

5 J. E. Bateman, J. F. Connolly, R. Stephenson, M. Edwards, J. C. Thompson, "The Development of Gas Microstrip Detectors for High Energy Physics Applications," Nucl. Instrum. Meth. A348 (1994) 372-377.

6 B. D. Ramsey, J. J. Kolodziejczak, M. A. Fulton, J.A. Mir and M.C. Weisskopf, "The development of Microstrip Proportional Counters for X-ray Astronomy," SPIE, Vol. 2280, (1994)110-118.

7 C. Budtz-Jorgensen, C. Olesen, H. W. Schnopper, T. Lederer, F. Scholze and G. Ulm, "The response functions of the HEPC/LEPC detector system measured at the Xe L edge region," Nucl. Instrum. Meth. A367(1995)83-87.

8 J. F. C. A. Veloso, J.A.M. Lopes, J. M. F. dos Santos and C. A. N. Conde, "A microstrip gas chamber as a VUV photosensor for a xenon gas proportional scintillation counter," to be published in IEEE Trans. Nucl. Sci.(1996)

9 Carl Butz-Jorgensen, A. Bahnsen, C. Olesen, M. M. Madesen, H. W. Schnopper and A. Oed, "Microstrip proportional counters for x-ray astronomy," Nucl. Instrum. Meth., A 310(1991) 82-87.

10 P. R. Bevington, "Data reduction and error analysis for the physical sciences," pp. 208-214. McGraw-Hill, New York (1969).

11 P. J. B. M. Rachinhas, T.H.V.T. Dias, A. D. Stauffer, F. P. Santos and C. A. N. Conde, "Energy Resolution of Xenon Proportional Counters: Monte Carlo Simulation and Experimental Results," presented at 1995 IEEE Nuclear Science Symposium, 21-28 October, San Francisco, USA. to be published in IEEE Trans. Nucl. Sci.(1996)

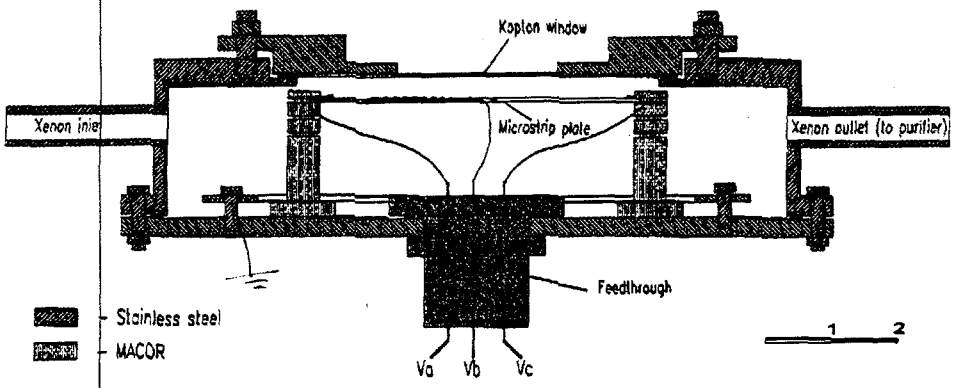
Kapton window
Xenon inlet
Microstrip plate
Xenon outlet (to purifier)
Feedthrough
Stainless steel
MACOR
Va
Vb
Vc
1
2

FIG. 1

1- error bars?
2- why imprecision in $\Delta E/E$ @ ~ Va ~ 425 ?
space charge effects? -

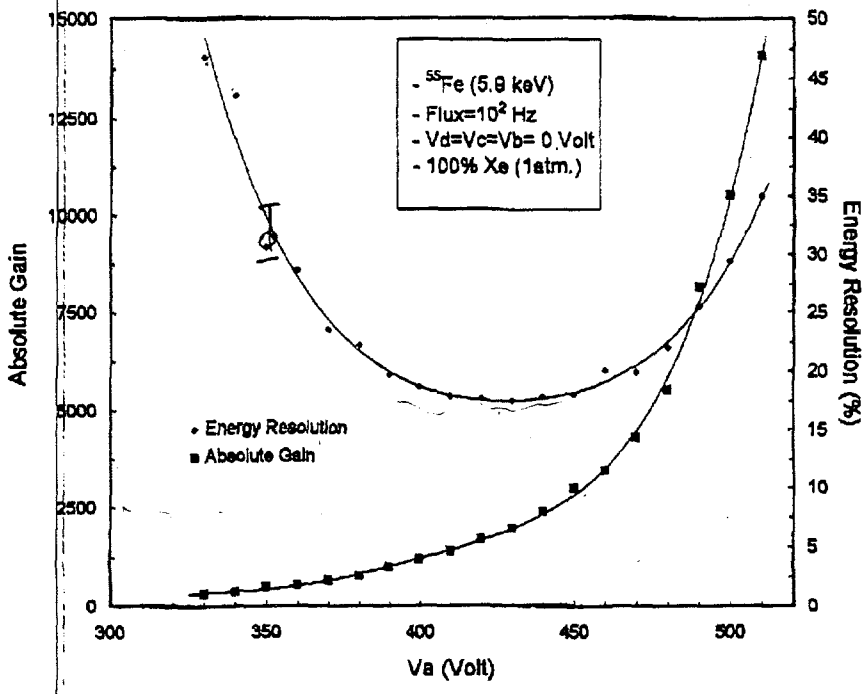

FIG. 2

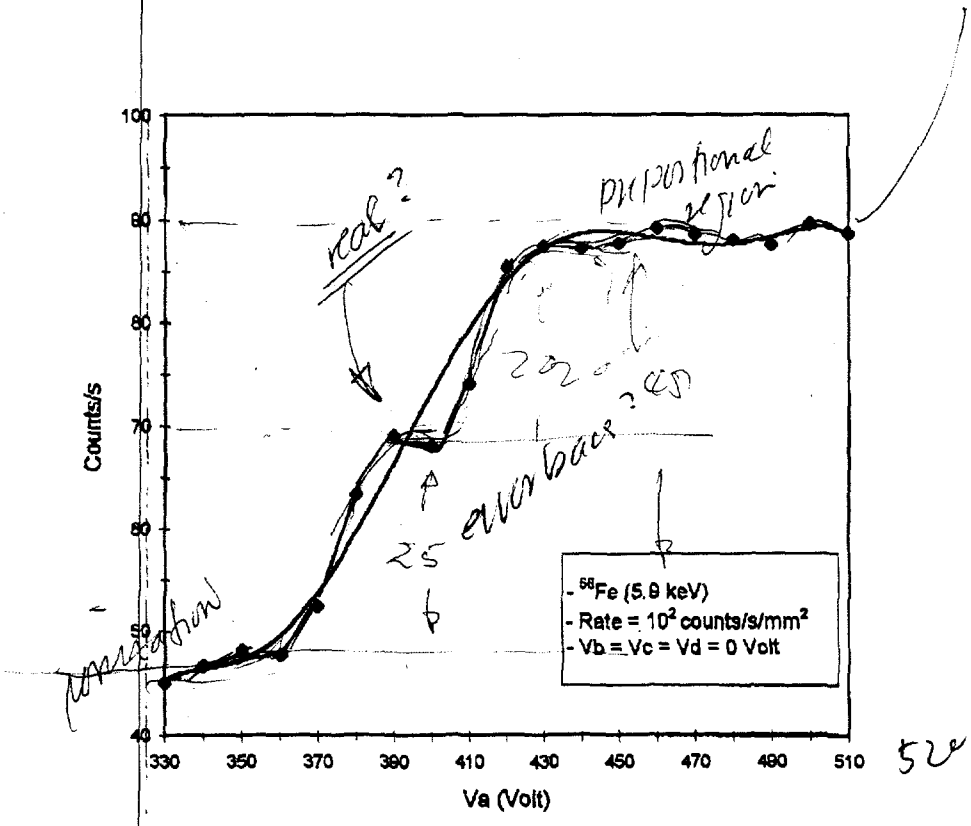
Counts/s
Ve (Volt)
- ^{55}Fe (5.9 keV)
- Rate = 10^2 counts/s/mm^2
- Vb = Vc = Vd = 0 Volt

Fig 3

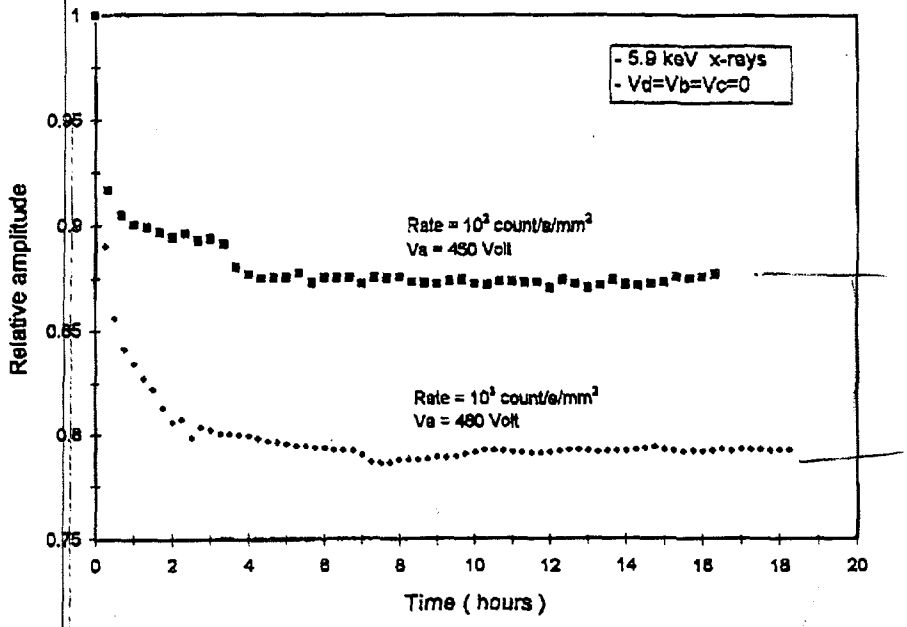

Do both these curves reach the same amplitude at equilibrium or ~~under~~

Fig. 4 the 10^3 curve really have a smaller amplitude?

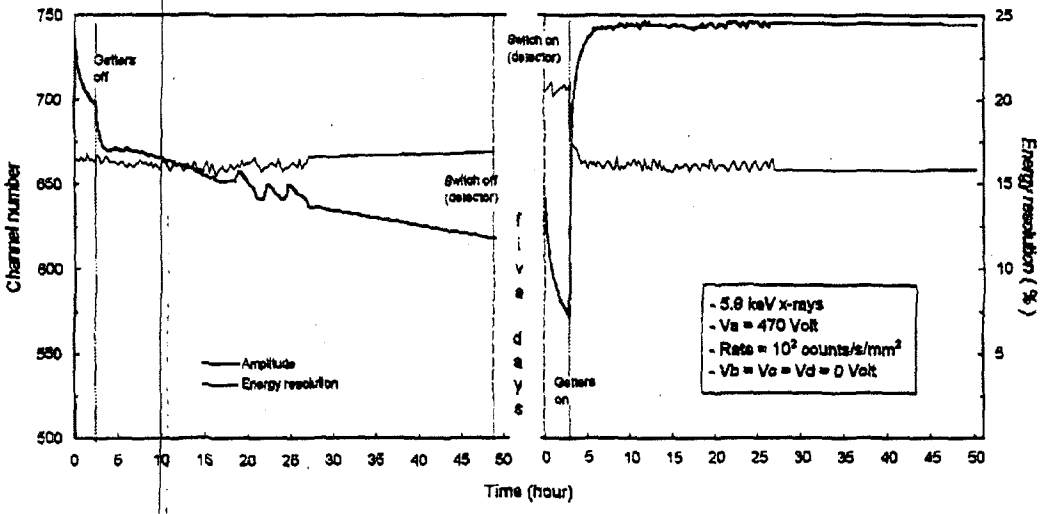
Getters off
Switch off (detector)
Switch on (detector)
Getters on
five days
Amplitude
Energy resolution
- 5.8 keV x-rays
- Va = 470 Volt
- Rate = 10² counts/s/mm²
- Vb = Vc = Vd = 0 Volt
Channel number
Energy resolution (%)
Time (hour)

Fig. 5.

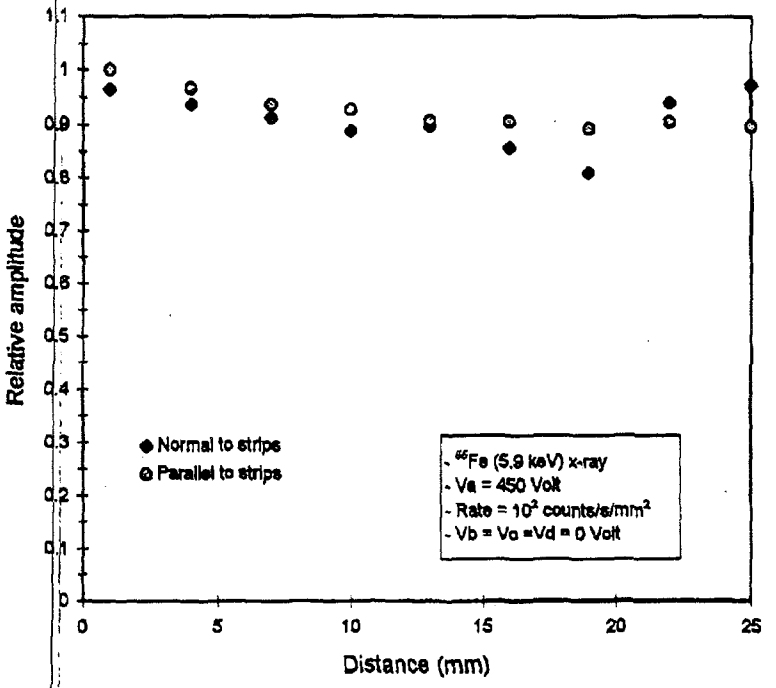
Relative amplitude
Distance (mm)
Normal to strips
Parallel to strips
- 55Fe (5.9 keV) x-ray
- Va = 450 Volt
- Rate = 10² counts/s/mm²
- Vb = Vc =Vd = 0 Volt

Fig. 6

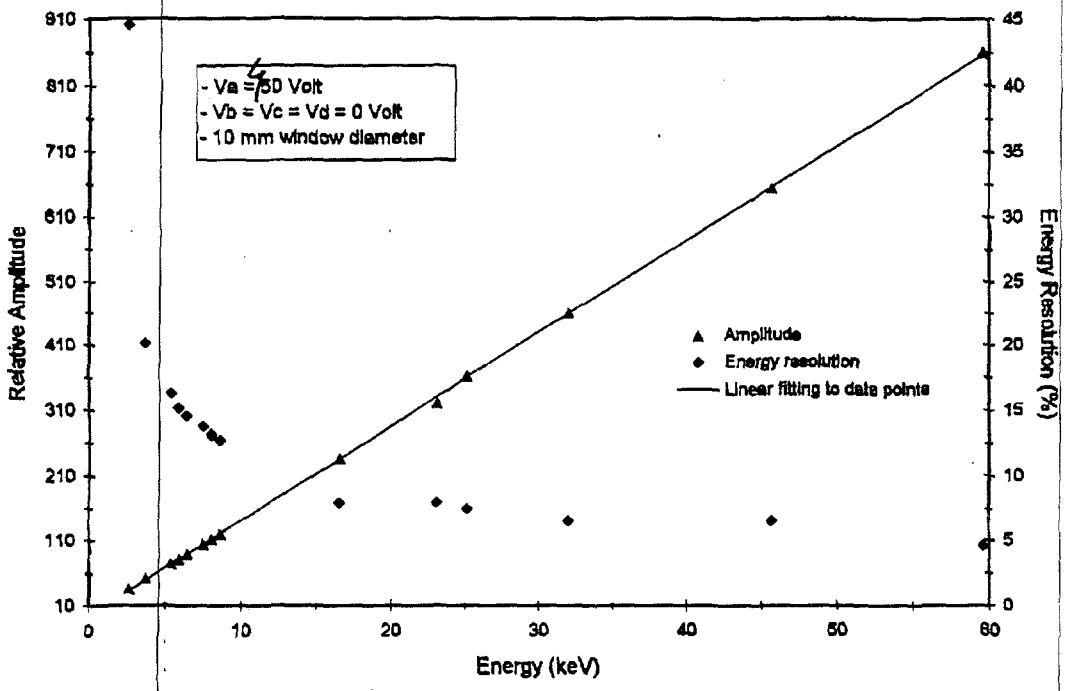
- Va = 50 Volt
- Vb = Vc = Vd = 0 Volt
- 10 mm window diameter
Amplitude
Energy resolution
Linear fitting to data points
Relative Amplitude
Energy Resolution (%)
Energy (keV)
910
810
710
610
510
410
310
210
110
10
45
40
35
30
25
20
15
10
5
0
0
10
20
30
40
50
60

Fig 7

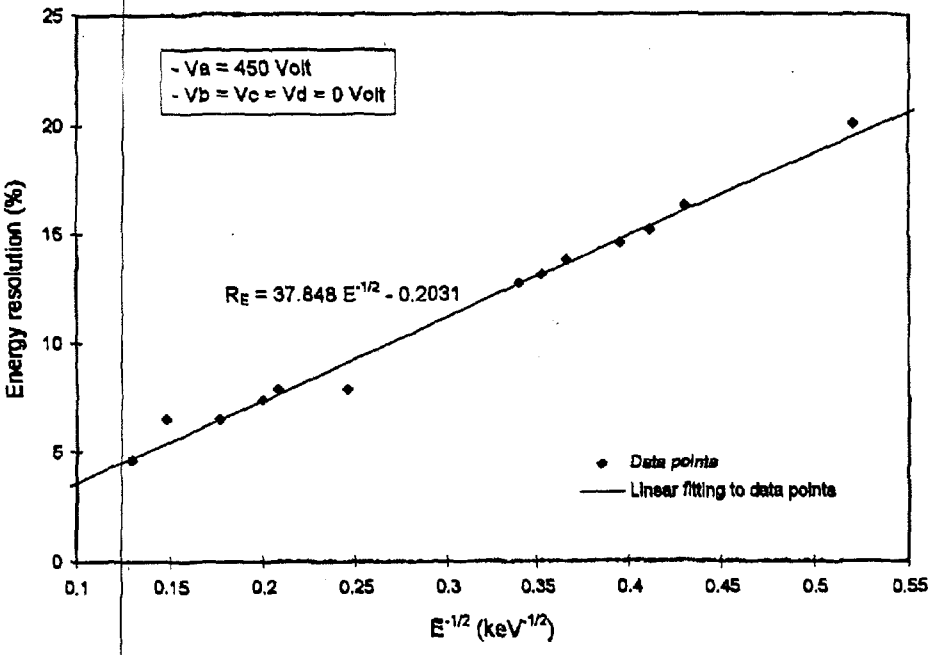
- Va = 450 Volt
- Vb = Vc = Vd = 0 Volt
$R_E = 37.848\ E^{-1/2} - 0.2031$
Data points
Linear fitting to data points
Energy resolution (%)
$E^{-1/2}$ (keV$^{-1/2}$)
0
5
10
15
20
25
0.1
0.15
0.2
0.25
0.3
0.35
0.4
0.45
0.5
0.55

Fig 7A

MTA9.XLS

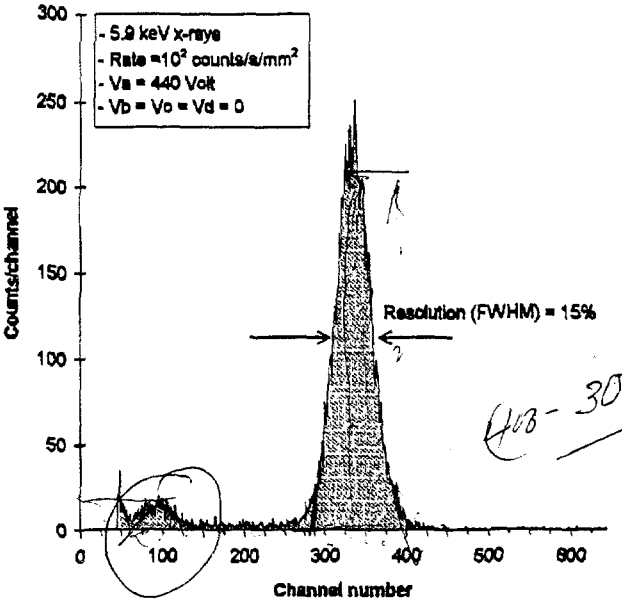

$A = \frac{(400 - 300) \times 200}{2} = 10^4$

$A' = \frac{60 \times 20}{2} \sim 600$

$\frac{600}{10000} \sim 6\%$

Fig 8a)

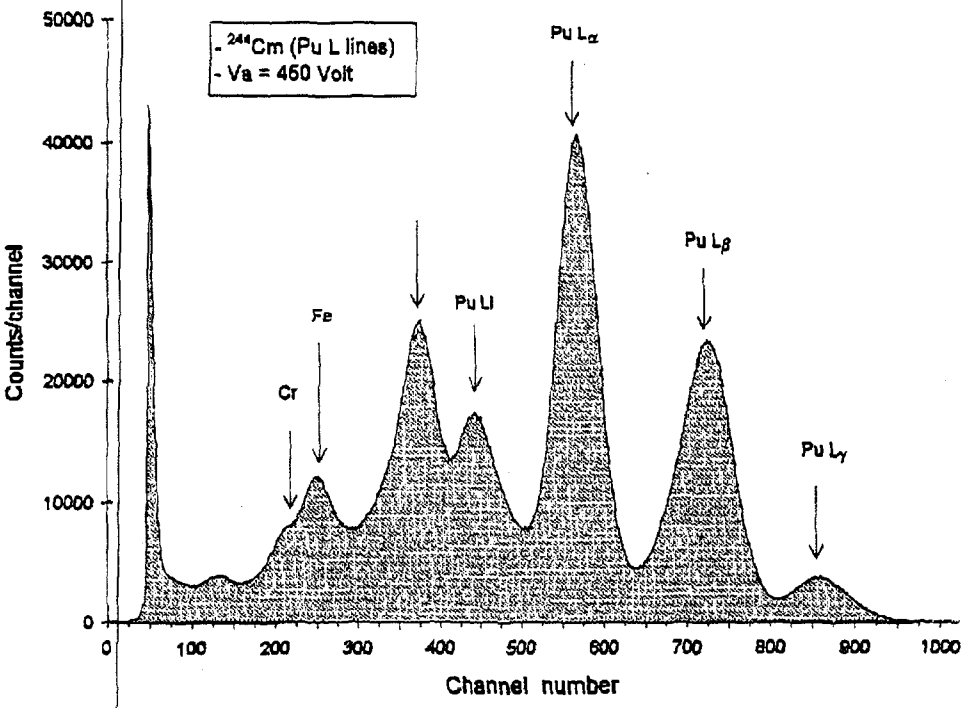
- ^{244}Cm (Pu L lines)
- Va = 460 Volt
Pu L_α
Pu L_β
Pu L_γ
Pu Ll
Fe
Cr
Counts/channel
Channel number
0
10000
20000
30000
40000
50000
0
100
200
300
400
500
600
700
800
900
1000

Fig 8

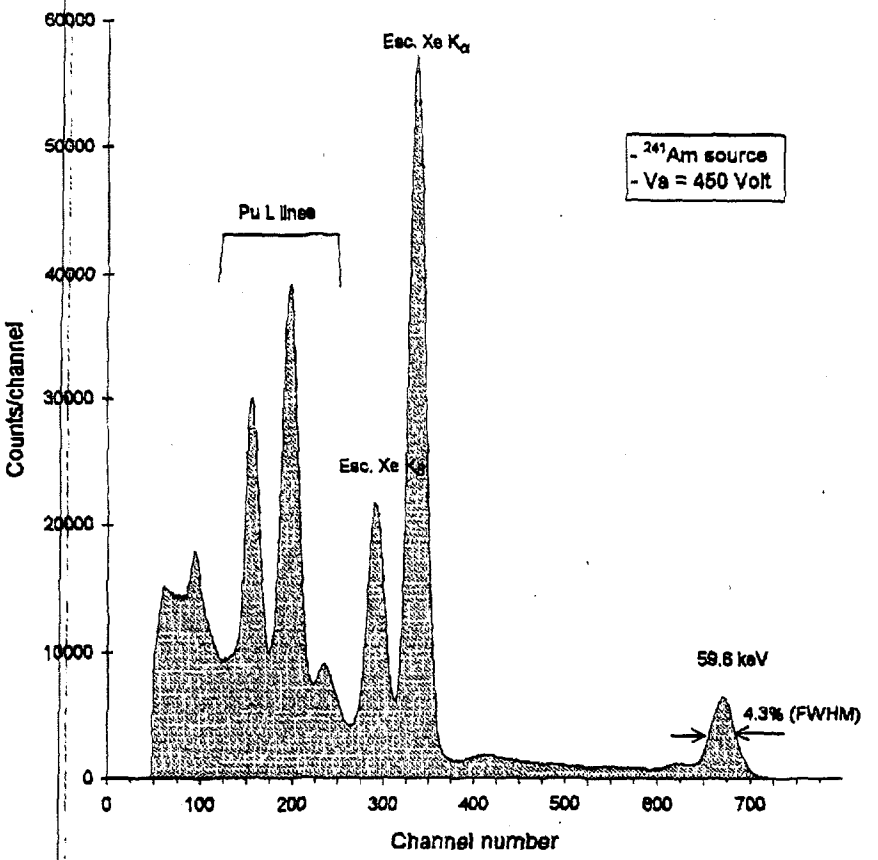
Esc. Xe K_α
- ^{241}Am source
- Va = 450 Volt
Pu L lines
Esc. Xe K_β
59.6 keV
4.3% (FWHM)
Counts/channel
Channel number
60000
50000
40000
30000
20000
10000
0
0
100
200
300
400
500
600
700

Fig 8.6)

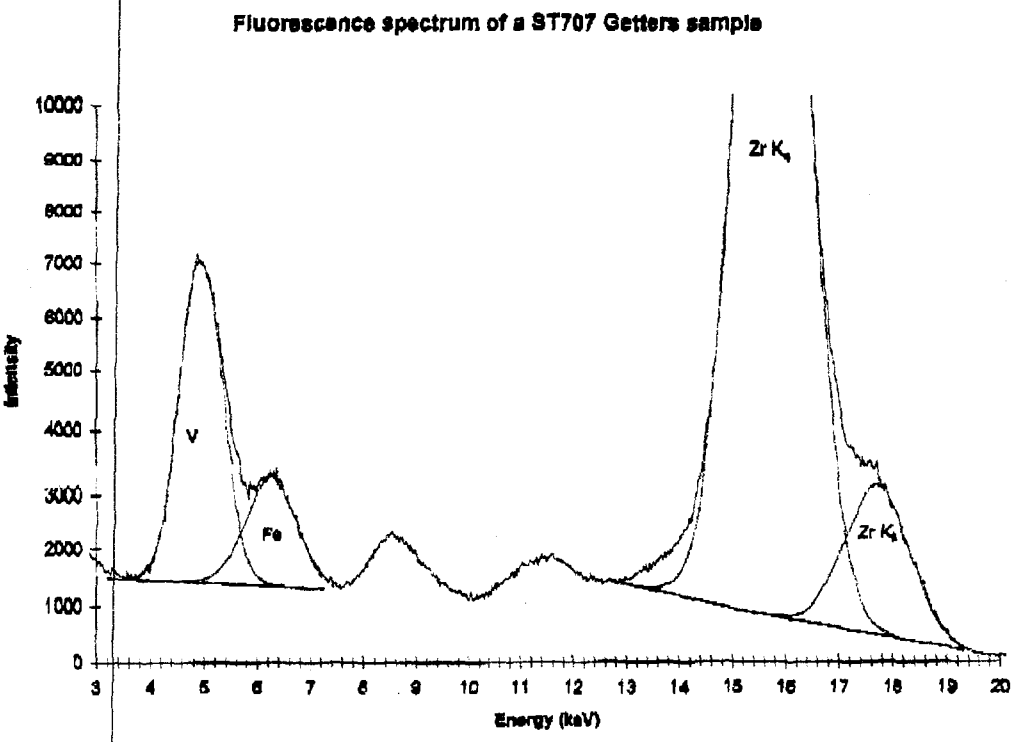
Fluorescence spectrum of a ST707 Getters sample
Intensity
10000
9000
8000
7000
6000
5000
4000
3000
2000
1000
0
3
4
5
6
7
8
9
10
11
12
13
14
15
16
17
18
19
20
Energy (keV)
V
Fe
Zr K$_\alpha$
Zr K$_\beta$

Sheet1 Chart 1

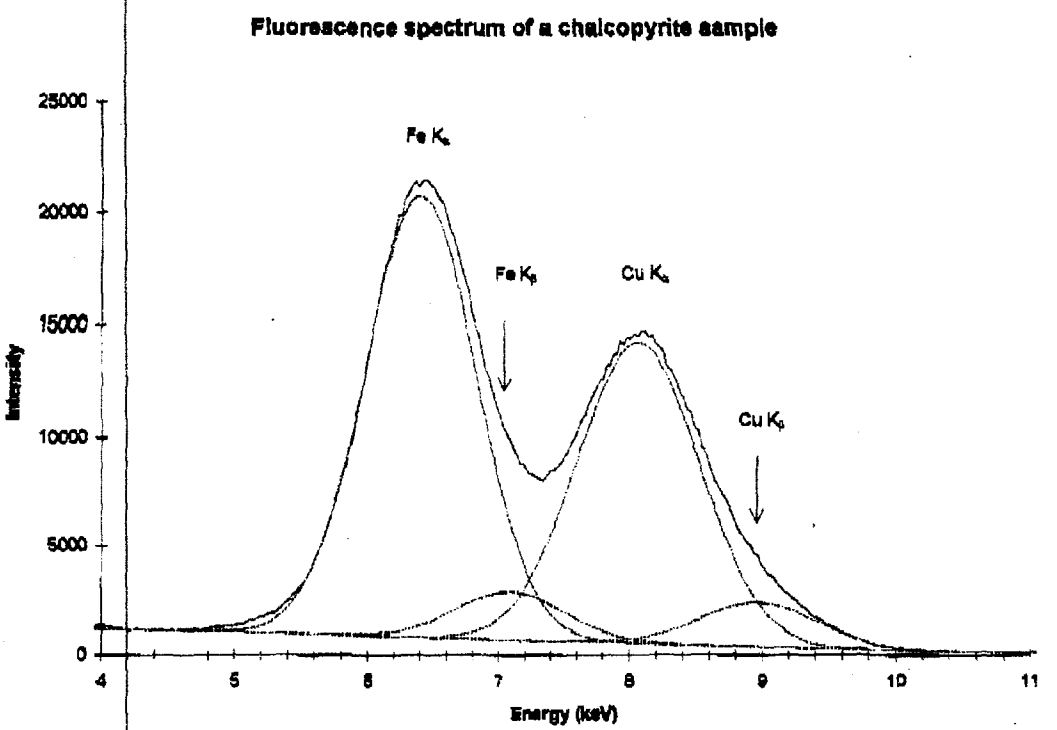

Sheet1 Chart 1

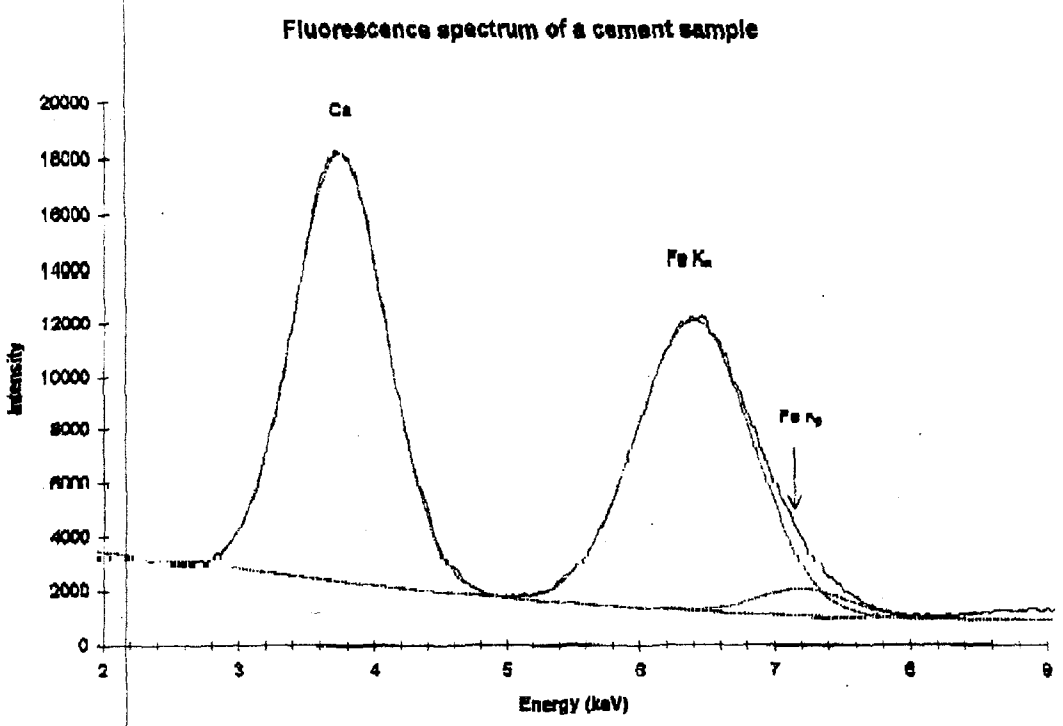

Sheet1 Chart 1

Fluorescence spectrum of a lead sample

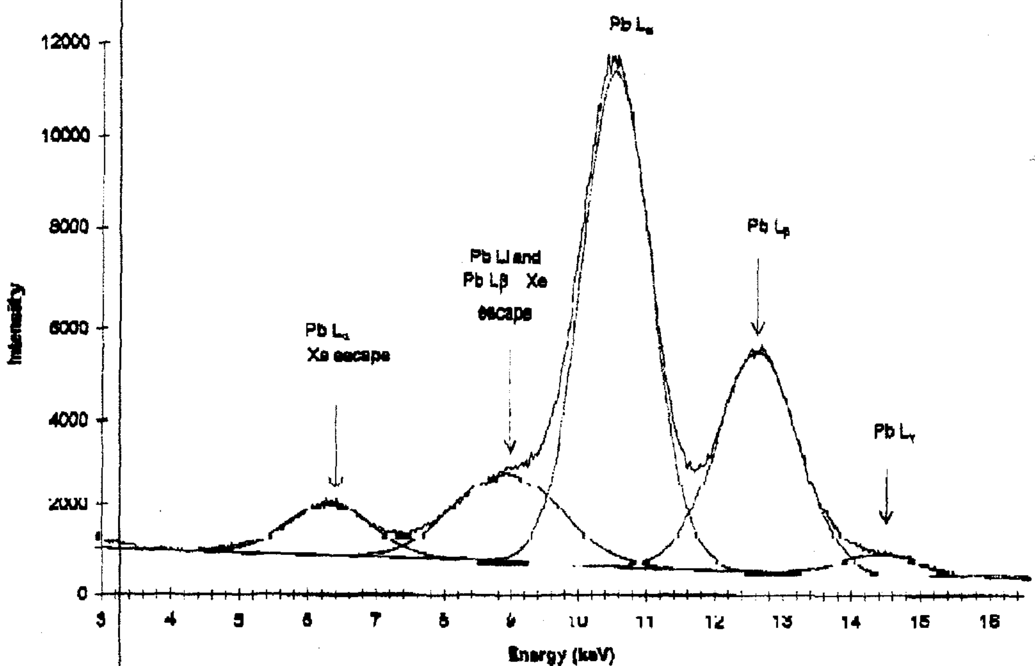

Sheet1 Chart 1